Journal of Biomechanics 48 (2015) 217–223

Contents lists available at ScienceDirect

Journal of Biomechanics

journal homepage: www.elsevier.com/locate/jbiomech
www.JBiomech.com

Biomechanical study on the bladder neck and urethral positions: Simulation of impairment of the pelvic ligaments

Sofia Brandão [a,*], Marco Parente [b], Teresa Mascarenhas [c], Ana Rita Gomes da Silva [c], Isabel Ramos [a], Renato Natal Jorge [c]

[a] Department of Radiology, Centro Hospitalar de São João—EPE, Faculty of Medicine, University of Porto, Alameda Prof. Hernâni Monteiro, 4200-319 Porto, Portugal
[b] IDMEC, Faculty of Engineering, University of Porto, Rua Dr Roberto Frias, s/n, 4200-465 Porto, Portugal
[c] Department of Gynecology and Obstetrics, Hospital de S. João, Faculty of Medicine, University of Porto, Alameda Prof. Hernâni Monteiro, 4200-319 Porto, Portugal

ARTICLE INFO

Article history:
Accepted 28 November 2014

Keywords:
Pelvic floor dysfunction
Biomechanical simulation
Finite element method
Soft tissue analysis
Ligament impairment

ABSTRACT

Excessive mobility of the bladder neck and urethra are common features in stress urinary incontinence. We aimed at assessing, through computational modelling, the bladder neck position taking into account progressive impairment of the pelvic ligaments.

Magnetic resonance images of a young healthy female were used to build a computational model of the pelvic cavity. Appropriate material properties and constitutive models were defined. The impairment of the ligaments was simulated by mimicking a reduction in their stiffness.

For healthy ligaments, valsalva maneuver led to an increase in the α angle (between the bladder neck-symphysis pubis and the main of the symphysis) from 91.8° (at rest) to 105.7°, and 5.7 mm of bladder neck dislocation, which was similar to dynamic imaging of the same woman (α angle from 80° to 103.3°, and 5 mm of bladder neck movement). For 95% impairment, they enlarged to 124.28° and 12 mm. Impairment to the pubourethral ligaments had higher effect than that of vaginal support (115° vs. 108°, and 9.1 vs. 7.3 mm).

Numerical simulation could predict urethral motion during valsalva maneuver, for both healthy and impaired ligaments. Results were similar to those of continent women and women with stress urinary incontinence published in the literature. Biomechanical analysis of the pubourethral ligaments complements the biomechanical study of the pelvic cavity in urinary incontinence. It may be useful in young women presenting stress urinary incontinence without imaging evidence of urethral and muscle lesions or organ descend during valsalva, and for whom fascial damage are not expected.

1. Introduction

Stress urinary incontinence (SUI) and organ prolapse (Patel et al., 2007) have a significant negative impact on quality-of-life. The pathophysiology is multifactorial, including aging, hormonal changes from menopause, vaginal delivery and high parity, often in consequence of nerve, muscle or ligament direct injury, pelvic fascia or ligament collagen degradation (Patel et al., 2007).

As experimental work in vivo is very hard to implement, imaging evidence and biomechanical modelling (Dietz, 2004; Yip et al., 2014) have illustrated the role of striated pelvic floor muscles defects in urinary (in)continence and organ support. While they act by means of passive and active forces (Chamochumbi et al., 2012), the pelvic fascia and ligaments provide additional passive stabilization (Brandão and Ianez, 2013). Evaluating ligament biomechanics according to tissue *status* is relevant to understand SUI features.

Previous computer modelling focused on the normal pelvic mobility (Cosson et al., 2013). Also, in the context of pelvic organ prolapse, the vaginal and vesical position was evaluated considering muscle and apical support weakening and impairment (Chen et al., 2006, 2009; Yip et al., 2014). Results suggest that the extent of anterior vaginal prolapse is related to the degree of both muscle and uterosacral–cardinal support impairment. Simulating 90% and 60% of ligament and pubovisceral muscle impairment, respectively, led to a threefold increase in vaginal prolapse, which explains the vesico-urethral descent.

The role of (ab)normal apical support on vesical position is in this way modelled. However, to our knowledge, the role of pubourethral ligaments (PUL) was never included in such analysis.

Abbreviations: ATFP, arcus tendineous fasciae pelvis; IAP, intra-abdominal pressure; PUL, pubourethral ligaments; SUI, stress urinary incontinence

* Corresponding author. Tel.: +351 96 4089922.
E-mail addresses: Sofia.brand@gmail.com (S. Brandão), mparente@fe.up.pt (M. Parente), rita.mgs89@gmail.com (A.R.G. da Silva), iramos@med.up.pt (I. Ramos), rnatal@fe.up.pt (R.N. Jorge).

http://dx.doi.org/10.1016/j.jbiomech.2014.11.045
0021-9290/

The PUL are important urethral stabilizers that insert on the posterior surface of the pubic bone (El-Sayed et al., 2007; Kim et al., 2003; Petros, 1998), as shown on Fig. 1(a and b). When they suffer from injury or laxity (c–e), an increase in the retropubic space, bladder neck funneling and urethral hypermobility may occur (Pregazzi et al., 2002). As a result, "complaint of any involuntary loss of urine on effort (…)", as defined by the International Continence Society, may occur during events that result in increased intra-abdominal pressure (see Fig. 1f)—as for example, sneezing, coughing, defecating or during physical exercise. This is a common finding in patients suffering from SUI (Kim et al., 2003; Pregazzi et al., 2002).

In what concerns UI, and from a functional aspect, the PUL are critical structures, along with the paraurethral and vaginal tissue and the *levator ani* muscle. The structural degradation of the support structures such as the ligaments and fascia can be another ingredient to develop SUI, as stated by the Integral Theory (Petros and Woodman, 2008). If the mechanical properties of the ligaments induce their laxity, the backward force against the PUL and the downward force against the uterosacral and cardinal ligaments during valsalva may prevent muscles from effectively pushing the urethra against the pubic bone. On the other hand, injury models in rats such as urethrolysis or PUL transection have reproduced trauma, and results showed urethral hypermobility and long-term SUI (Kefer et al., 2008). For these reasons, by modelling the joint action of the PUL along with the apical support may add information on its contribution to (ab)normal bladder neck and urethral mobility, which are findings in young women presenting SUI, but with no evidence of organ prolapse or muscle damage.

Accordingly, the purpose of this work was to model, under a mechanical perspective, the effect of distinct levels of ligament impairment. For this purpose, we measured the bladder neck mobility and the changes in the α angle for valsalva maneuver using live subject MRI and a computational model based on the Finite element method.

2. Materials and methods

2.1. Subject and imaging

The Institutional Review Board approved this work (protocol: CES195/12).

A nulliparous 24-year female with no complains of pelvic dysfunction was the volunteer for the scanning session. A gynecologist observed her and no morphologic or functional abnormalities were found.

The volunteer was instructed on how to perform correct valsalva maneuver at two different time-points. First, a trained nurse and the gynecologist gave full instructions during clinic observation. Second, the nurse and an experienced physiotherapist on pelvic floor rehabilitation gave additional support during the scanning session. Several attempts were performed with the volunteer lying in the scanner table before the beginning of the acquisitions.

Magnetic resonance images were acquired in the supine position at rest using a 3.0 T system (Magnetom® Tim Trio, Siemens Medical Solutions, Erlangen, Germany) equipped with two (anterior and posterior) 6ch-phased-array RF coils. The woman lied in supine position with legs together in a semiflexed position.

Multiplanar pelvic high-resolution T2w fast spin-echo (FSE) images were obtained (TE/TR 96/3860 ms; 2 mm slices (no interslice gap); field-of-view 26 cm; matrix 384 × 384 and 3 NSA (number of signals averaged).

Additional dynamic images were obtained in the mid-sagittal plane, approximately every 1.6 s for 30 s using a half-Fourier acquisition single-shot turbo spin-echo (HASTE) pulse sequence (TE/TR 96/1600 ms; 6 mm slices; field-of-view 28 cm, matrix: 155 × 256 and 1 NSA).

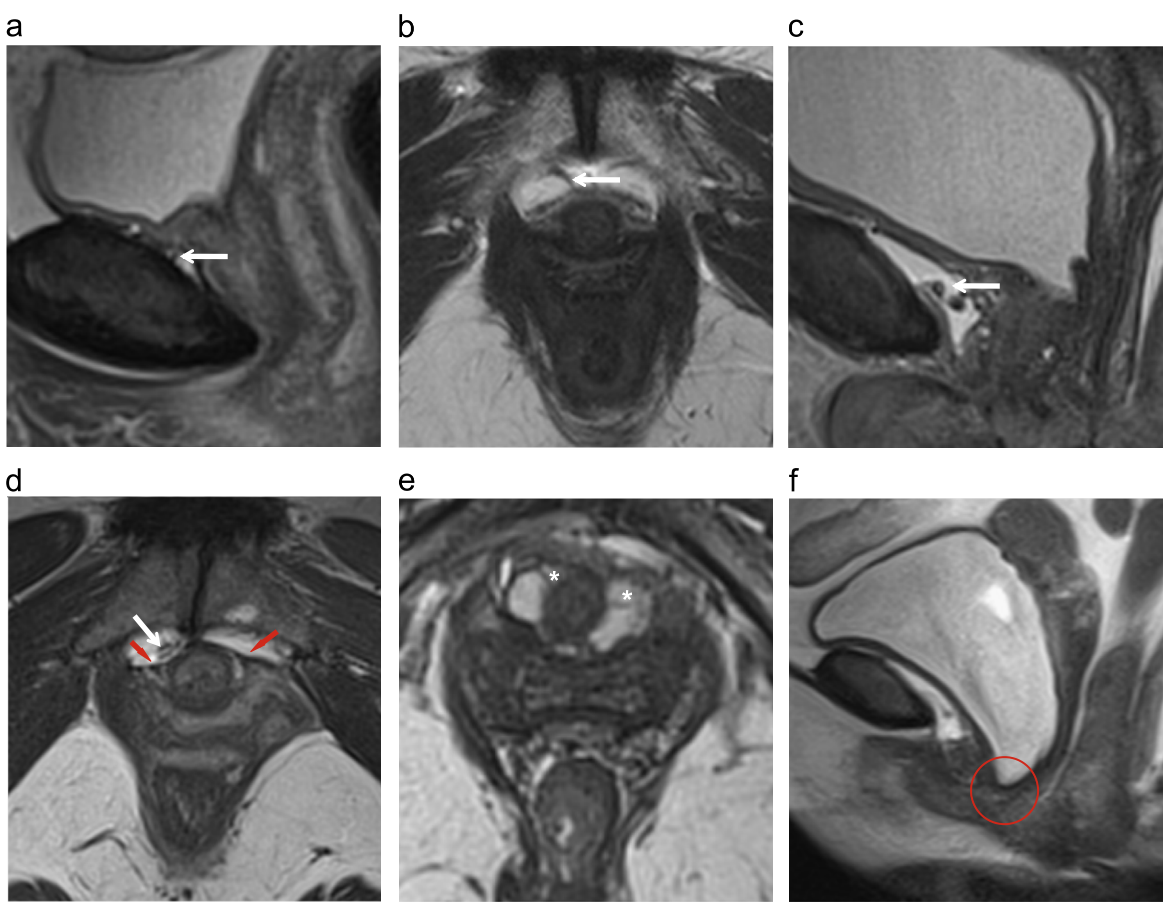

Fig. 1. Magnetic resonance imaging (MRI) of the support to the urethra and bladder. The pubourethral ligaments are thin hypointense bands that attach the bladder neck to the symphysis pubis. They can be seen in sagittal (a) and axial high-resolution images (b) (white arrow). Some women with stress urinary incontinence (SUI) show ligament distortion (c) and (d), and increased retropubic space. The position of urethra may not be maintained, as the peri- and paraurethral ligaments (red arrows on (d)) and (asterisks on (e), respectively) are not stretched tight, and urethral rotation may occur. Urethral hypermobility and bladder neck funneling (red circle on (f)) are shown during valsalva maneuver. (For interpretation of the references to color in this figure legend, the reader is referred to the web version of this article.)

During the dynamic scanning, 2 images were acquired at rest during suspended inspiration (approximately 3 s), 5 during minimal, 5 during moderate and 5 during maximal valsalva (total of 24 s), and the last 2 during normal breathing (approximately 3 s). Three sets of these 19 successive images were acquired 3 times with 2 min interval. The best maximal valsalva image was selected for analysis. It was chosen by measuring the most evident vertical descent of the bladder neck along a horizontal axis drawn at the outer side of the *periosteum* in the inferior edge of the pubic bone, and simultaneously having the wider hiatal sagittal diameter.

The radiologist observed all the images, and no suspicious findings were reported.

2.2. Finite element model

The high-resolution T2w images were used to identify and segment several anatomical structures. Two readers (20 and 15 years experience) *in consensus* confirmed anatomical landmarks. To create the 3D solid model (see Fig. 2) the axial images were imported to the Inventor® software (Autodesk, San Raphael, CA, USA), and the structures were outlined with contour splines. This solid geometry was then discretized into a finite element mesh with tetrahedral elements using the Abaqus® software v.6.12 (Dassault Systèmes Simulia Corp., Providence, RI, USA).

The finite element model included the bony pelvis, the pelvic organs, and some of the main supporting structures (the *levator ani* muscle, the pubourethral, uterosacral, cardinal and the lateral ligaments of the rectum, the pubocervical fascia and the *arcus tendineous fasciae pelvis* (ATFP)). Although we did not expect a direct influence of the lateral ligaments of the rectum on the bladder neck and urethral position, they were included as posterior compartment supporters. The width and length of the lateral ligaments of the rectum (1.5 cm and 2.2 cm, respectively) were confirmed in the literature (Lin et al., 2010). The ATFP length (9.0 cm) was measured by its attachment points and compared with cadaver dissection data (Albright et al., 2005; Occelli et al., 2001); further geometric details were retrieved from the literature (Albright et al., 2005; Pit et al., 2003). Fig. 2 illustrates the 3D model with all the structures considered for the modelling and simulation.

For the modelling, the organs were described as having hyperelastic mechanical behaviour while the bones were fixed and considered as rigid (Dalstra et al., 1993).

As pelvic cavity soft tissues such as muscles and ligaments are composed by fibers that are aligned with their main anatomical and functional axis, we used simple isotropic models adjusted to the main direction of these structures. For that purpose, the Yeoh (1993) and Ogden (1972) constitutive equations were used to model the behaviour of all the soft tissues. The pelvic fascia was assumed as having similar mechanical properties to those of the abdominal fascia (Kirilova et al., 2011). Table 1 presents the constitutive parameters. The material properties were obtained from previous publications using experimental data from female cadaver without pelvic floor dysfunction (Cosson et al., 2003; Janda, 2006; Martins et al., 2011; Rivaux et al., 2013; Rubod et al., 2012). The curve-fitting algorithm from Abaqus® was applied to each experimental dataset. During the fitting process, the model that better adjusted the experimental data was chosen by determining the correlation coefficient (r) between the different curves. Fig. 3 shows the experimental and numerical curves, as well as the correlation coefficient, that were obtained for each tissue.

The supporting structures were attached to the organs and bone by using multi-point constrains (Abaqus® tie). The nodes corresponding to the pubic bone and the extremities of the *levator ani* muscle, pelvic fascia, PUL and anterior portion of the ATFP that attach to the pubic bone were fixed. The same boundary conditions were applied to the insertion of the lateral ligaments of the rectum in the endopelvic fascia, to the sacral attachment of the uterosacral ligaments, to the postero–lateral connection of the *levator ani* in the *arcus tendineous of the levator ani*, and to the cardinal ligament insertion in the obturator fascia. The interaction between the organs was modelled as frictionless, and established using the default Abaqus® contact pressure-overclosure algorithm.

The model was tested using Abaqus® Standard for pressure values that correspond to the IAP for supine rest and supine valsalva maneuver, following the methodology described by Noakes et al. (2008). Despite the fact that the supine position does not mimic the normal physiologic state, the model was built from MR images acquired in the supine position, and therefore the same conditions should be established. Since the muscles already incorporate resting tone in the supine position, the mean pressure at rest (0.5 kPa) was subtracted from the average supine valsalva pressure (4.5 kPa) to obtain the value of 4 kPa.

For those values of pressure, mean values of displacement of the pelvic organs and pelvic floor muscles were evaluated considering all the ligaments as healthy so as to validate the numerical model. Furthermore, in order to have a starting point to evaluate the effect of simulating changes in stiffness of the ligaments, two common measures of vesico-urethral mobility were tested at rest and for valsalva maneuver. The bladder neck mobility was assessed according to the standardized x–y coordinate system described by Schaer et al. (1995) by setting the same reference axis on Abaqus®. A line passing the axis of the symphysis pubis (x-axis) intercepted a second line perpendicular to this to cross at the infero-posterior margin of the symphysis pubis (y-axis). The position of the bladder neck at rest and valsalva maneuver was then defined. The α angle was also evaluated as described by Pregazzi et al. (2002), by measuring the angle between the bladder neck and the symphysis pubis, and the x-axis.

In a second stage, we simulated the valsalva meneuver while considering impairment to all the ligaments, and also considering the anterior, middle and posterior support ligaments. Structural impairment was simulated by reducing material stiffness. Fig. 4 shows the behavior assumed for the impaired ligaments, which were achieved by multiplying the stress/strain curve of a healthy ligament obtained from a uniaxial tension tests (Rivaux et al., 2013) by a given coefficient (0.75, 0.50, 0.25 and 0.05). The new datasets were imputed in the curve-fitting algorithm from Abaqus® software, and new parameters were obtained (numerical curves in Fig. 4). Since we focused exclusively on changing stiffness of the ligaments, we decided to keep the other structures (including organs) intact. The primary outcomes of this second stage were again the α angle and the bladder neck dislocation to compare with the ones of the first simulation.

3. Results

We found that the value of IAP affects the position of the pelvic structures.

Fig. 5 shows the displacement maps that evidence the movement of the pelvic organs and pelvic floor muscles at rest (a) and when simulating valsalva maneuver (b), considering all ligaments as healthy. To better illustrate the displacement, their contour was outlined (c). Dynamic MRI (d) at valsalva is also seen. Results from numerical simulation showed that the uterus, bladder and the rectal portion of the pelvic floor evidenced the highest displacement. The pelvic floor muscles showed an inferior and posterior displacement of 6.1 and 1.6 mm, respectively. Accordingly, the rectum descended 3.7 mm. The uterus went down 10.7 mm further compressing the body of the bladder (9.1 mm) against the pubic bone. This led to a slight posterior movement of the urethra and vagina (0.5 and 0.8 mm, respectively).

In the numerical simulation, the α angle and the bladder neck dislocation varied according to the two conditions. When considering

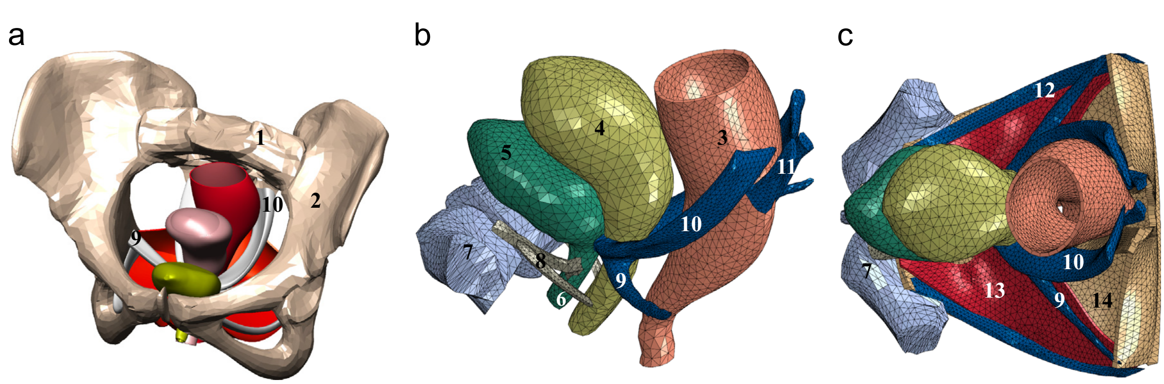

Fig. 2. Anatomical perspective of the 3D model. The pelvic bones, organs and several soft tissue support structures were included (a). In (b) and (c), some of the osseous structures were hidden for a better visualization of the soft tissues. ((1) sacrum; (2) bony pelvis; (3) rectum; (4) uterus; (5) bladder; (6) urethra; (7) symphysis pubis; (8) pubourethral ligaments; (9) cardinal ligaments (10) uterosacral ligaments; (11) lateral ligaments of the rectum; (12) *arcus tendineous fasciae pelvis*; (13) pelvic fascia; (14) pelvic floor muscles).

Table 1
Material properties and hyperelastic constitutive models for the structures included in the model.

Structure	α_k	μ_k	–	Model	Experimental data
Bladder and urethra	$\alpha_1=0.19$	$\mu_1=5.14$	–	Ogden ($N=1$)	Martins et al. (2011)
Rectum	$\alpha_1=4.25$	$\mu_1=13.24$	–	Ogden ($N=2$)	Rubod et al. (2012)
	$\alpha_2=-3.83$	$\mu_2=13.24$	–		
Vagina and uterus	$\alpha_1=-3.41$	$\mu_1=92.24$	–	Ogden ($N=3$)	Rubod et al. (2012)
	$\alpha_2=-0.66$	$\mu_2=39.29$	–		
	$\alpha_3=-6.48$	$\mu_3=54.68$	–		
Pelvic fascia and ligaments (ATFP, CL, LLR, USL)	$\alpha_1=10.85$	$\mu_1=3.17$	–	Ogden ($N=1$)	Rivaux et al. (2013)
Pelvic ligaments (PUL)	$\alpha_1=10.95$	$\mu_1=1.58$	–	Ogden ($N=1$)	Rivaux et al. (2013)
	C_{10}	**C_{20}**	**C_{30}**	**Model**	
Pubocervical fascia	0.93	−0.62	0.47	Yeoh	Kirilova et al. (2011)
Pelvic floor muscles	0.003	0.002	0.001	Yeoh	Janda, (2006)

α_k and μ_k—material constants.
ATFP—*arcus tendineus fascia pelvis*; CL—cardinal ligaments; PUL—pubourethral ligaments; LLR—lateral ligaments of the rectum; USL—uterosacral ligaments.

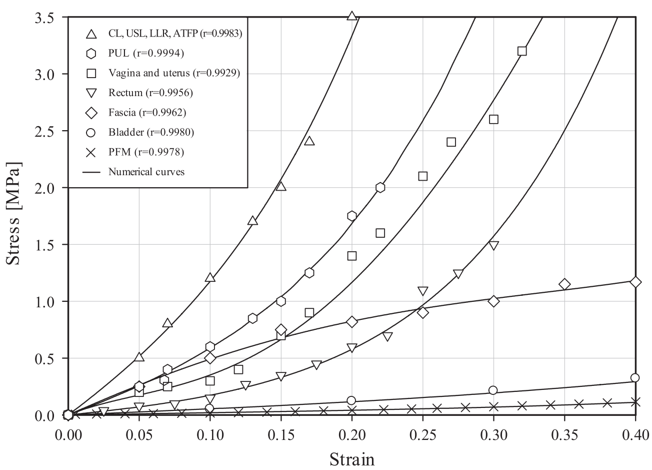

Fig. 3. Fitting process to obtain the material properties for the different tissues included in the model. The experimental and numerical curves are shown. For each tissue, the model that better fitted the experimental data was chosen. (CL—cardinal ligaments; USL—uterosacral ligaments; LLR—lateral ligaments of the rectum; ATFP—*arcus tendineous fasciae pelvis*; PUL—pubouretral ligaments; PFM—pelvic floor muscles).

the ligaments as healthy, valsalva maneuver opened the α angle from 91.8° to 105.7° and the bladder neck moved 5.7 mm posteriorly. Measures taken in the MR images revealed similar values: the α angle changed from 88° to 103.3° and the bladder neck dislocation was 5 mm.

Fig. 6 shows that at valsalva maneuver progressive ligament impairment increases these values, except for the lateral ligaments of the rectum. Between 75% and 95% impairment, a pronounced effect was produced when the impairment was applied to all the ligaments simultaneously, and also for the PUL. Isolated impairment to the PUL resulted in a more evident increase of the bladder neck angle and urethral mobility than damage on the apical vaginal supporters (115° vs. 108°, and 9.1 mm vs. 7.3 mm).

Fig. 7 displays the bladder and urethra contours. A dot was drawn in the region of the bladder neck to illustrate its position. The grey continuous line represents the bladder neck at rest. It changes from 91.8° to 108.7° and moves 6.9 mm for valsalva maneuver considering there has been 50% of impairment to all the ligaments (grey dashed line), and 124.3° and moves 12 mm for a 95% impairment (black continuous line).

4. Discussion

This paper presents a live MRI-based model used to investigate the effect of simulating impairment of the pelvic ligaments in the α angle and the bladder neck mobility during valsalva maneuver, which is often evaluated through diagnostic imaging for women suffering from SUI. Results of numerical simulation were in agreement with dynamic MRI of the same woman, and also with what was reported by Pregazzi et al. (2002) for asymptomatic women (91.8° and 88° vs. 92 ± 6° at rest, 105.7° and 103.3° vs. 100 ± 8° at valsalva). Simulation of impairment on all ligaments revealed an α angle similar to what was described by the same author for incontinent women (124.3° vs. 120 ± 8° at valsalva). Results for bladder neck dislocation are also similar to what was previously described by Peschers et al. (2001) and Howard et al. (2000) (14 ± 9 mm (ranging from 2 mm to 31 mm) and 12.4 ± 4.7 mm, respectively) for continent, and by Viereck et al. (2006) for incontinent women (13.7 mm, ranging from 2 mm to 30 mm). The minor differences between our results from numerical simulation and MRI may be related to the pressure applied. We cannot assure that they were exactly the same, despite the volunteer was instructed on how to perform correct valsalva maneuver. Nevertheless, the value of IAP was correct according to the woman's position in the MR scanner. Still, a different pressure would result in more or less dislocation of the bladder neck and urethra. This can also explain the differences between our results and the literature, as previous studies report a wide range of values that may result from patient cooperation and awareness on performing valsalva maneuver.

Fig. 6 shows that when all the ligaments were considered as impaired, an evident increase in the α angle and bladder neck mobility were seen for valsalva maneuver. The pelvic organs are distensible structures with attachments that allow for normal mobility, which would not be possible with fixed rigid ligaments. Because changes in mechanical strength are dependent on morphology and mechanical properties of the tissue, our results suggest similar results published for the apical ligaments, that is the interrelationship between the impairment of these support structures and their biomechanical behavior. Decreasing ligaments stiffness induces excessive mobility, and therefore when impaired ligaments are tensioned, they will suffer higher deformations that lead to increased urethral mobility.

In our model, the PUL seem to have the greatest effect on the position of the bladder neck. As shown on Fig. 6, if we impose an impairment of 95% of the PUL – that is considering them as almost absent – while maintaining the material properties of the uterine and rectal support ligaments constant, we can recognize that the dynamics of the pelvic cavity measured at the anterior compartment is highly changed. This may be related to their attachment on the midurethra, which explains that injury causes further descent than the one obtained for the apical ligaments.

Deficiency on the PUL is directly associated with the mechanism of urethral hypermobility (Kefer et al., 2008), as severe lesions decrease the leak point pressure, which is likely to lead to loss of urine during cough or exercise. Besides urethral hypermobility,

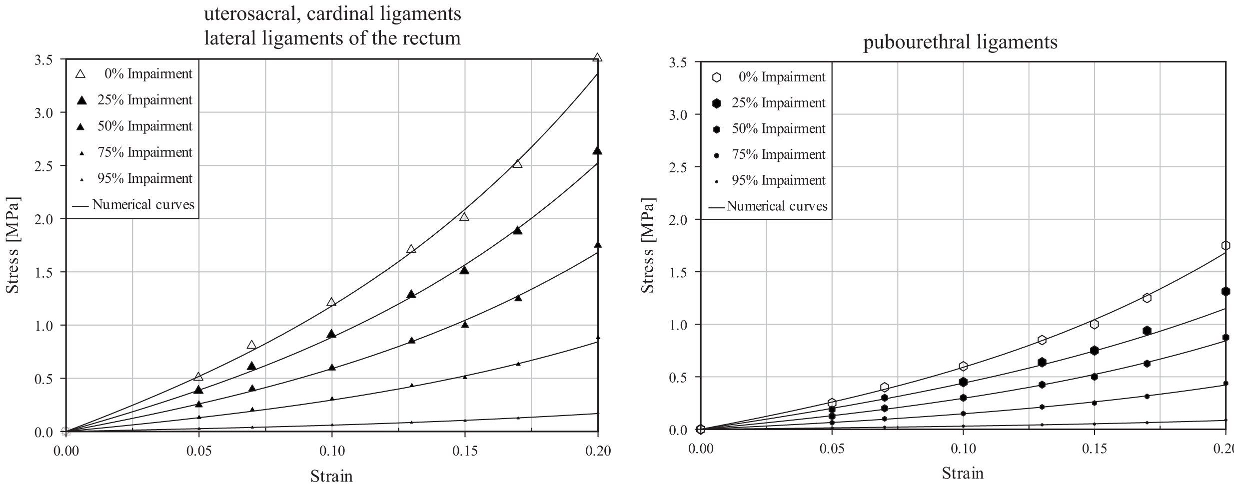

Fig. 4. Numerical curves obtained from Abaqus® software.

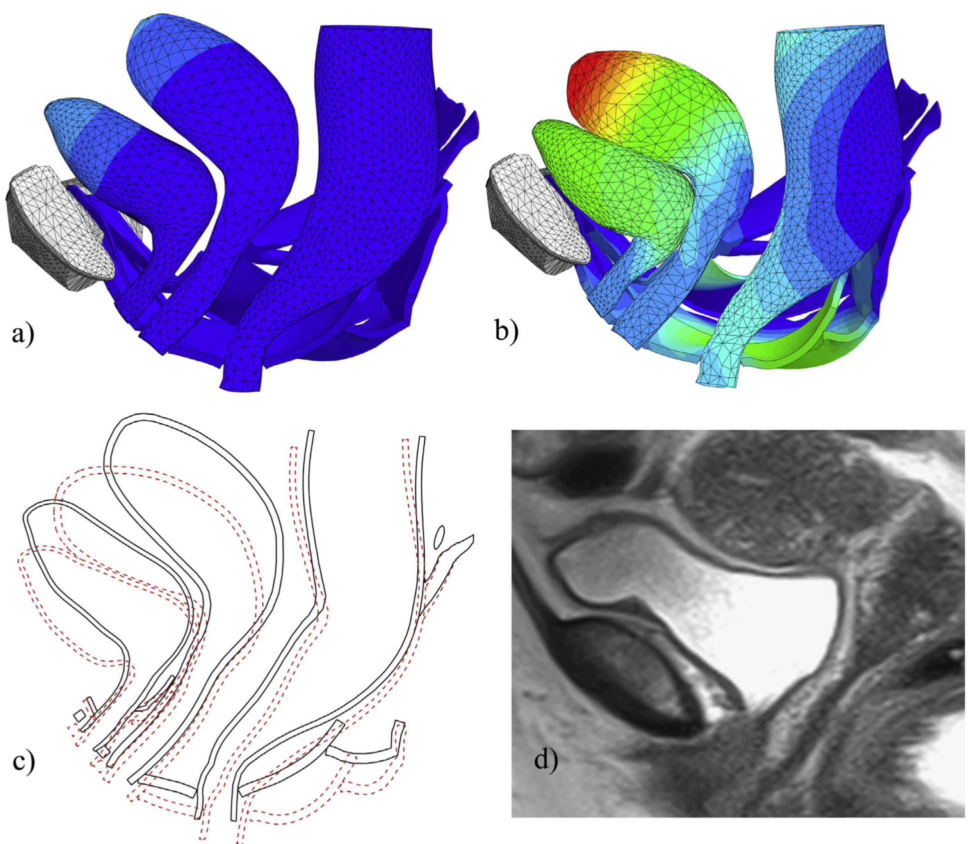

Fig. 5. Pelvic organs and muscles displacement at rest (a) and for valsalva maneuver (b) considering the ligaments as healthy. The body of the uterus, the bladder and the rectal portion of the pelvic floor muscles evidenced the highest displacement. In (c), their contours at rest (black continuous lines) and valsalva maneuver (red dashed lines) were drawn. (For interpretation of the references to color in this figure legend, the reader is referred to the web version of this article.)

other passive mechanisms such as intrinsic sphincter deficiency or abnormal urethral compliance, and also insufficient voluntary contraction of the pelvic muscles may contribute to SUI.

Despite the fact that this model was build based in only one women, this subject-specific Finite Element modelling approach has the potential for application to patient- or patient group-based MRI datasets. It would be helpful in young women presenting SUI but with imaging evidence of normal urethral and muscle anatomy, and pelvic organ positioning during dynamic ultrasound or MRI, for whom fascial damage are not expected. Likewise, prediction of surgical trauma during bladder neck suspension procedures or urethral diverticulectomy could be helpful to adjust the surgical approach for a patient-specific situation. This provides a means to examine the biomechanics of the pelvis for cases where the woman's morphology is a key issue, such as patients with previous hysterectomy due to changes in normal dynamics between anterior and middle compartment, or when the pelvic floor muscles are very thin or are slightly disrupted and thus start reducing their active support. We believe that it could also be applied to future modelling of excessive fetal head compression to the bladder and urethra against the pubis during labor, which would elucidate on the causes for post-partum SUI.

a

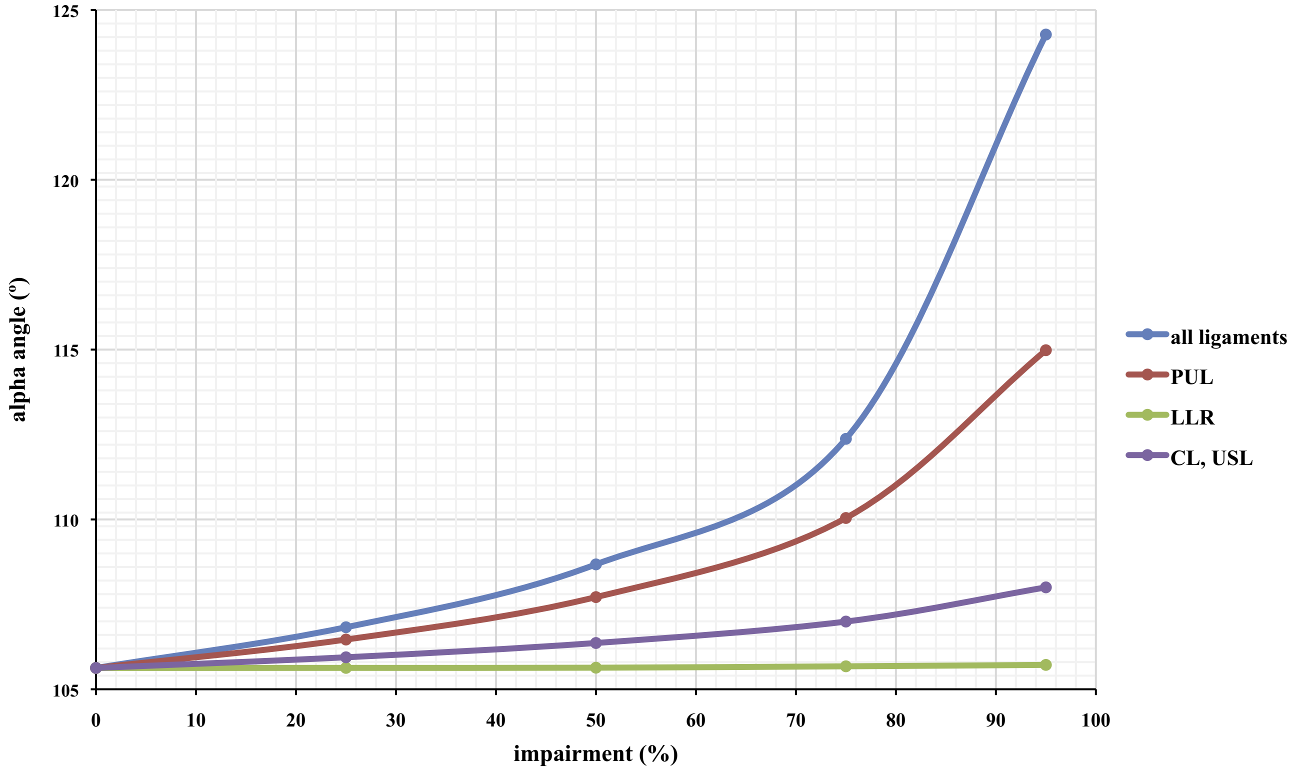

b

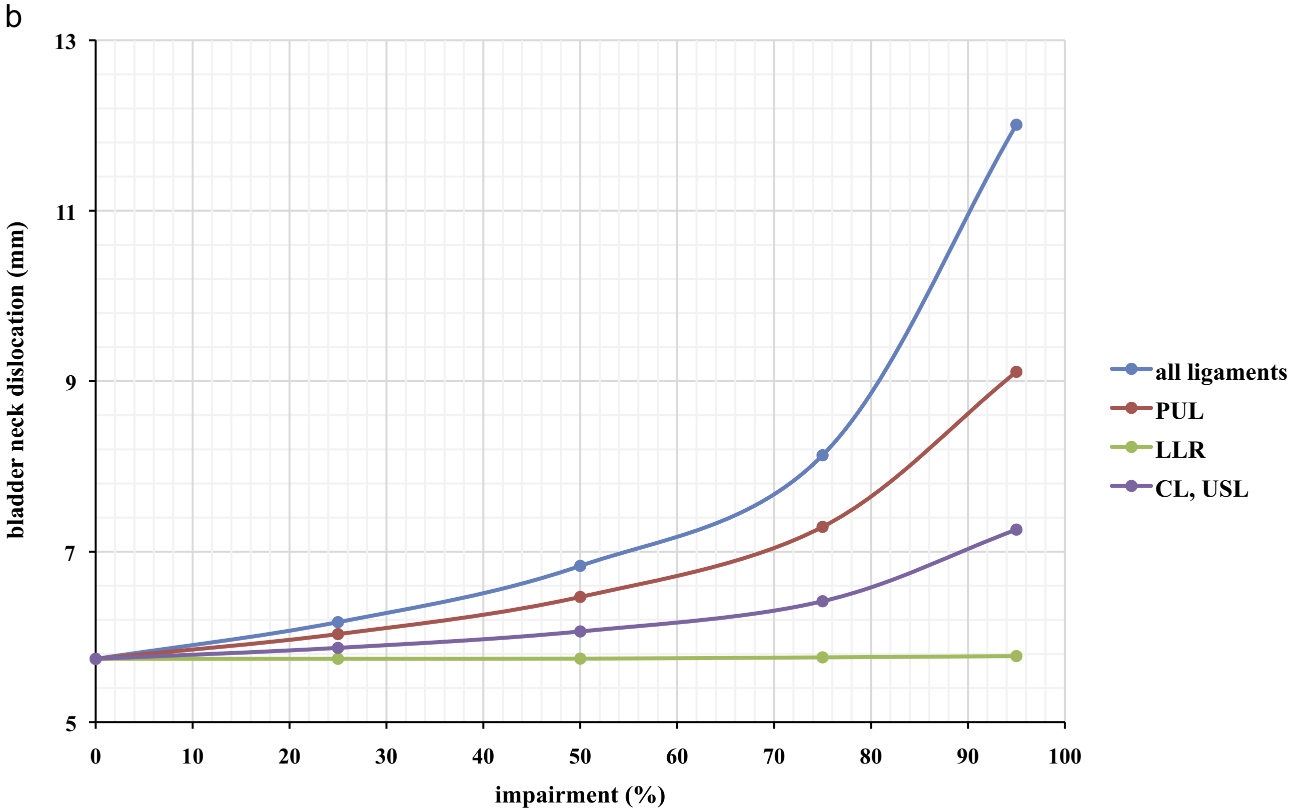

Fig. 6. Values of the α angle (a) and bladder neck dislocation (b) according to the increased impairment of the pelvic ligaments. When considered alone, the impairment of the pubourethral ligaments led to the highest increase on the α angle and bladder neck dislocation. (CL—cardinal ligaments; LLR—Lateral ligaments of the rectum; PUL—pubouretral ligaments; USL—uterosacral ligaments).

There are certain limitations in this study. First, not all the pelvic ligaments were considered in this model. The urethral support does rely not only on the PUL but also on the pubovesical, the periurethral and the paraurethral ligaments. We have chosen to include only the PUL for several reasons: to simplify the model, due to their relevance to the urethral and vaginal anchoring, and

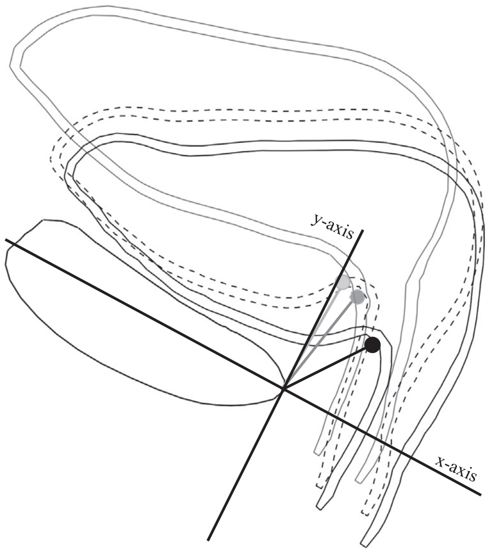

Fig. 7. Variation of the position of the bladder neck.

also the existing evidence of their disruption in SUI patients. Second, the pelvic floor muscles were modelled as a single structure having the same thickness, which is not entirely correct, as the puborectal portion of the *levator ani* is usually thicker. Third, both the MRI acquisitions and modelling were performed considering the supine position, which does not mimic the normal physiologic state, as coughing, exercising, or defecating are performed in the upright or sitting positions. For that purpose simulation of standing valsalva comparing with standing MRI would be interesting. Nevertheless, one may assume that standing up implies higher IAP values.

In spite of the limitations noted, we feel that this model is a step forward in the biomechanical analysis of SUI. These simulations showed the central contribution of the PUL to maintain the bladder neck position.

In conclusion, we presented a biomechanical model that predicted the effect of the position of pelvic organs in real-life circumstances.

Financial disclamer/conflict of interest statement

The authors disclose financial and personal relationships that could inappropriately influence this work.

Funding

The authors acknowledge the funding of the project PEst-OE/EME/LA0022/2013, from Fundação da Ciência e Tecnologia, Portugal and to the project "Biomechanics: contributions to the healthcare", reference NORTE-07-0124-FEDER-000035 co-financed by Programa Operacional Regional do Norte (ON.2—O Novo Norte), through the Fundo Europeu de Desenvolvimento Regional (FEDER).

References

Albright, T.S., Gehrich, A.P., Davis, G.D., Sabi, F.L., Buller, J.L., 2005. *Arcus tendineus fascia pelvis*: a further understanding. Am. J. Obstet. Gynecol. 193 (3 Pt 1), 677–681. http://dx.doi.org/10.1016/j.ajog.2005.02.129.

Brandão, AC, Ianez, P., 2013. MR imaging of the pelvic floor: defecography. Magn. Reson. Imaging Clin. N. Am 21 (2), 427–445. http://dx.doi.org/10.1016/j.mric.2013.01.007.

Chamochumbi, CC., Nunes, FR., Guirro, RR., Guirro, EC., 2012. Comparison of active and passive forces of the pelvic floor muscles in women with and without stress urinary incontinence. Rev. Bras. Fisioter. 16 (4), 314–319. http://dx.doi.org/10.1590/S1413-35552012005000020.

Chen, L., Ashton-Miller, J.A., DeLancey, J.O., 2009. A 3D finite element model of anterior vaginal wall support to evaluate mechanisms underlying cystocele formation. J. Biomech. 42 (10), 1371–1377. http://dx.doi.org/10.1016/j.jbiomech.2009.04.043.

Chen, L., Ashton-Miller, J.A., DeLancey, J.O., Hsu, Y., 2006. Interaction between apical supports and *levator ani* in anterior vaginal support: theoretical analysis. Obstet. Gynecol. 108 (2), 324–332. http://dx.doi.org/10.1097/01.AOG.0000227786.69257.a8.

Cosson, M., Boukerrou, M., Lacaze, S., Lambaudie, E., Fasel, J., Mesdagh, H., Lobry, P., Ego, A., 2003. A study of pelvic ligament strength. Eur. J. Obstet. Gynecol. Reprod. Biol 109 (1), 80–87. http://dx.doi.org/10.1016/S0301-2115(02)00487-6.

Cosson, M., Rubod, C., Vallet, A., Witz, J.F., Dubois, P., Brieu, M., 2013. Simulation of normal pelvic mobilities in building an MRI-validated biomechanical model. Int. Urogynecol. J. 24 (1), 105–112. http://dx.doi.org/10.1007/s00192-012-1842-8.

Dalstra, M., Huiskes, R., Odgaard, A., van Erning, L., 1993. Mechanical and textural properties of pelvic trabecular bone. J. Biomech. 26 (4–5), 523–535.

Dietz, H.P., 2004. Ultrasound imaging of the pelvic floor. Part II: Three-dimensional or volume imaging. Ultrasound Obstet. Gynecol. 23, 615–625. http://dx.doi.org/10.1002/uog.1072.

El-Sayed, R.F., Morsy, M.M., El-Mashed, S.M., 2007. Anatomy of the urethral supporting ligaments defined by dissection, histology, and MRI of female cadavers and MRI of healthy nulliparous women. AJR Am. J. Roentgenol 189 (5), 1145–1157.

Howard, D., Miller, J.M., Delancey, J.O., Ashton-Miller, J.A., 2000. Differential effects of cough, valsalva, and continence status on vesical neck movement. Obstet. Gynecol. 95 (4), 535–540.

Janda, S., 2006. Biomechanics of the Pelvic Floor Musculature (Ph.D. Thesis Dissertation). Delft University of Technology (ISBN:90.9020334).

Kefer, J.C., Liu, G., Daneshgari, F., 2008. Pubo-urethral ligament transection causes stress urinary incontinence in the female rat: a novel animal model of stress urinary incontinence. J. Urol. 179 (2), 775–778.

Kim, J.K., Kim, Y.J., Choo, M.S., Cho, K.S., 2003. The urethra and its supporting structures in women with stress urinary incontinence: MR imaging using an endovaginal coil. AJR Am. J. Roentgenol 180 (4), 1037–1044. http://dx.doi.org/10.2214/ajr.180.4.1801037.

Kirilova, M., Stoytchev, S., Pashkouleva, D., Kavardzhikov, V., 2011. Experimental study of the mechanical properties of human abdominal fascia. Med. Eng. Phys. 33 (1), 1–6. http://dx.doi.org/10.1016/j.medengphy.2010.07.017.

Lin, M., Chen, W., Huang, L., Ni, J., Yin, L., 2010. The anatomy of lateral ligament of the rectum and its role in total mesorectal excision. World J. Surg. 34 (3), 594–598. http://dx.doi.org/10.1007/s00268-009-0371-1.

Martins, P.A., Filho, A.L., Fonseca, A.M., Santos, A., Santos, L., Mascarenhas, T., Jorge, RM., Ferreira, A.J., 2011. Uniaxial mechanical behavior of the human female bladder. Int. Urogynecol. J. 22 (8), 991–995. http://dx.doi.org/10.1007/s00192-011-1409-0.

Noakes, K.F., Pullan, A.J., Bissett, I.P., Cheng, L.K., 2008. Subject specific finite elasticity simulations of the pelvic floor. J. Biomech. 41 (14), 3060–3065. http://dx.doi.org/10.1016/j.jbiomech.2008.06.037.

Ogden, R.W., 1972. Large deformation isotropic elasticity—on the correlation of theory and experiment for incompressible rubberlike solids. Proc. R. Soc. London, Ser. A 326 (1567), 565–584.

Occelli, B., Narducci, F., Hautefeuille, J.P., Querleu, D., Crépin, G., Cosson, M., 2001. Anatomic study of arcus tendineus fasciae pelvis. Eur. J. Obstet. Gynecol. Reprod. Biol 97 (2), 213–219.

Patel, P.D., Amrute, K.V., Badlani, G.H., 2007. Pelvic organ prolapse and stress urinary incontinence: a review of etiological factors. Indian J. Urol 23 (2), 135–141. http://dx.doi.org/10.4103/0970-1591.32064.

Peschers, U.M., Fanger, G., Schaer, G.N., Vodusek, D.B., DeLancey, J.O., Schuessler, B., 2001. Bladder neck mobility in continent nulliparous women. BJOG 108 (3), 320–324. http://dx.doi.org/10.1111/j.1471-0528.2001.00066.x.

Petros, P.E., 1998. The pubourethral ligaments-an anatomical and histological study in the live patient. Int. Urogynecol. J. Pelvic Floor Dysfunct. 9 (3), 154–157.

Petros, P.E., Woodman, P.J., 2008. The integral theory of continence. Int. Urogynecol. J. 19, 35–40. http://dx.doi.org/10.1007/s00192-007-0475-9.

Pit, M.J., De Ruiter, M.C., Lycklama A Nijeholt, A.A., Marani, E., Zwartendijk, J., 2003. Anatomy of the arcus tendineus fasciae pelvis in females. Clin. Anat 16 (2), 131–137. http://dx.doi.org/10.1002/ca.10102.

Pregazzi, R., Sartore, A., Bortoli, P., Grimaldi, E., Troiano, L., Guaschino, S., 2002. Perineal ultrasound evaluation of urethral angle and bladder neck mobility in women with stress urinary incontinence. BJOG 109 (7), 821–827. http://dx.doi.org/10.1111/j.1471-0528.2002.01163.x.

Rivaux, G., Rubod, C., Dedet, B., Brieu, M., Gabriel, B., Cosson, M., 2013. Comparative analysis of pelvic ligaments: a biomechanics study. Int. Urogynecol. J. 24 (1), 135–139. http://dx.doi.org/10.1007/s00192-012-1861-5.

Rubod, C., Brieu, M., Cosson, M., Rivaux, G., Clay, J.C., de Landsheere, L., Babriel, B., 2012. Biomechanical properties of human pelvic organs. Urology 79 (4), 968e17–22. http://dx.doi.org/10.1016/j.urology.2011.11.010.

Schaer, G.N., Koechli, O.R., Schuessler, B., Haller, U., 1995. Perineal ultrasound for evaluating the bladder neck in urinary stress incontinence. Obstet. Gynecol. 85 (2), 224–229.

Viereck, V., Nebel, M., Bader, W., Harms, L., Lange, R., Hilger, R., Emons, G., 2006. Role of bladder neck mobility and urethral closure pressure in predicting outcome of tension-free vaginal tape (TVT) procedure. Ultrasound Obstet. Gynecol. 28, 214–220. http://dx.doi.org/10.1002/uog.2834.

Yeoh, O.H., 1993. Some forms of the strain energy functin for rubber. Rubber Chem. Technol. 66, 754–771.

Yip, C., Kwok, E., Sassani, F., Jackson, R., Cundiff, G., 2014. A biomechanical model to assess the contribution of pelvic musculature weakness to the development of stress urinary incontinence. Comput. Methods Biomech. Biomed. Eng. 17 (2), 163–176. http://dx.doi.org/10.1080/10255842.2012.672564.